OPTICAL LINKED RF INTERFEROMETER

By
Jun AMAGAI, Hiroo KUNIMORI, Hitoshi KIUCHI, and Koichi SEBATA

(Received on)

Keywords: Radio interferometer, Geodesy, Delay calibration, Optical link

Running Title: Optical linked RF Interferometer

ABSTRACT

Optical transmission in a fiber using modulation in the radio-frequency range with a delay compensation system (optical linked RF interferometer) were tested using the GMRT (Giant Meter-wave Radio Telescope in India) facility. The results of link budget measurement and delay compensation test show that the system is practicable for the interferometer with optical fiber cable of more than 20 km.

1. Introduction

A real-time data transmission system for the Very Long Baseline Interferometer (VLBI) network using an asynchronous data transfer mode (ATM) network has recently been implemented for the Keystone Project (KSP) [(1)], which now makes KSP VLBI's observation and analysis system fully automatic. Data productivity has been considerably improved and the estimation of the baseline lengths is now accurate to within a centimeter [(2)].

However, even greater accuracy in baseline estimation may be achieved by the introduction of a fiber optic link system for transmitting the radio frequency signal of the radio interferometer from an observation station to the analysis station, converting the frequency with a common local signal, and compensating for the delay occurring in the link [(3)]. Since a common local signal is used for converting the radio signal to a lower frequency and an unknown phase is not introduced into the observed phase, we can use phase delay instead of group delay and improve the accuracy of delay determination.

The performance of this fiber optic link system was checked only by using test signals and very short fiber optic cables. So we performed experiments to check the performance of the system by using the GMRT [(4)].

2. Optical Linked RF Interferometer

Fig. 1 shows the configuration of the optical-linked RF interferometer. A signal with a radio frequency (objective signal) is detected by an antenna at each observation site (Stations A and B), amplified by a low-noise amplifier (LNA), and converted to a 1310-nm optical signal by a laser diode (#1 or #2). The optical signals are transmitted through optical fibers to the analysis station, where they are reproduced as electrical signals (at #3 or #4). Common local signals (SG) are used to convert the reproduced signals to video signals, which are then processed by a correlation processor.

Delay changes that occur in the optical fibers are compensated for by calibration signals, which make a round trip between the analysis station and the observation sites. A radio-frequency calibration signal (cal. signal) is generated at the analysis station, converted to 1550-nm optical signal (#5), and divided into two signals by an optical power divider (#6). Then, each divided signal is transmitted using a wavelength division multiplexing (WDMs #7 or #8) to each observation site through the same optical fiber that feeds the objective signal. At each observation site the calibration signal is selected out again by a WDM (#9 or #10). By using an optical coupler with unequal divide ratio (#11, #12) we then divide the calibration signal into two optical signals with different intensities: a normal calibration signal and a reflected calibration signal. The normal calibration signal is converted to an electric signal at

the observation site (#17 or #18) and fed into the receiving system through a directional coupler installed just before the LNA. Although feeding the signal after the LNA is preferable to prevent contamination of the objective signal by optical receiver noise, feeding the signal before the LNA is necessary to compensate for the delay of the LNA. The normal calibration signal is processed as the phase calibration signal of a typical geodetic VLBI. The reflected calibration signal is directly reflected by an optical reflector and returns to the analysis station through the same optical fiber. At the analysis station, the reflected calibration signal is selected out by the WDM (#7 or #8) and fed to a photo detector (#15 or #16) via the optical directional coupler (#13 or #14). The reflected calibration signals converted to electric signals for both stations are converted to a lower frequency and processed in the same manner as the normal calibration signal.

We investigated the performance of optical linked RF interferometer [3]. According to the results of the investigation, we found from the signal-to-noise ratio analysis, that the practicable cable length is limited to 58.0 km by the link condition for the calibration signal. The results of preliminary experiments with this interferometer and short optical fiber lead to the following conclusions:

• Long-term delay fluctuation is less than 1 psec when the temperature of the system is kept within a 1-deg variation.

• The optical fiber delay is successfully compensated for (within an error of 100 psec for group delay and 1 psec for phase delay) by calibration signals in the radio-frequency range.

Although we demonstrated that we can determine the absolute delay not only for group delay but also for phase delay, we should note that it is difficult to use phase delay for an actual experiment where an objective signal passes through a dispersive medium because the phase delay does not directly correspond to the group delay in such a condition.

Note that our delay compensation method is available only for wavelength dispersion; polarization mode dispersion cannot be compensated for. Delay of up to about 8 psec [5] for a 58-km optical fiber cable, caused by polarization mode dispersion, remains even after we apply our delay compensation method.

3. Experiments

Optical transmitters and receivers were transported from the CRL to the GMRT and, they were installed, as shown in Fig. 2, in the GMRT system instead of the original optical equipment of the GMRT.

We used the interferometer elements S4 and S6 which are located at the south end of the GMRT (Fig. 3). The reason we selected S6 is that it is better to use long fiber cables to check our delay calibration system. The reason we selected S4 is that it is easier to get good fringes without resolving structures of radio stars by using a short baseline length.

The positions of the interferometer elements and the length of the optical fiber cables which connect the elements and central building are listed in Table 1.

Observed frequency was selected in 327 MHz band because of limitation of the instruments. The signal received by the receiver located on the prime focus of the antenna is amplified by a low-noise amplifier and led to the room just under the antenna via a low-loss

coaxial cable. In the room just under the antenna, the signal is fed to the optical transmitter and the converted optical signal is transmitted to the central building via the optical fiber cable of the GMRT.

At the central building, the electric signal is reproduced from the optical signal by using an optical receiver, converted to an IF signal (70 MHz), and then converted again to a video signal by using the facilities of the GMRT. The video signal is fed into the versatile digital-data-recorder (DDR).

The local signal generated by an oscillator is divided into two signals and fed to each receiving system. The video bandwidth was selected to be 64 kHz.

Comb tone is usually used for the delay calibration signal but we used a single tone for the experiment. The frequency of the tone signal is scanned synchronously with the local frequency of the video converter. The local frequency is selected to convert the delay calibration signal to 10 kHz.

The test experiments include the items described below.

1) Power level check of delay calibration signals.
We checked the power level of the delay calibration signals (both normal and reflected ones) which make the round trip between the central building and the antennas.

2) Delay calibration test
We recorded the calibration signals (both normal and reflected ones), which return from the two antenna sites, by using a digital data recorder (DDR) with a bandwidth of 24 kHz at the central building. The data were measured at 14 frequencies. The recording duration for each frequency was 30 sec.
From this experiment, we can determine the cable delay difference ; the difference of the time required for each signal traveling through the fiber optic cables connecting the antennas and central building. The error of this measurement is roughly estimated as follows [6]:

Phase determination error	σ_ϕ = 0.17 rad (10 deg.)
Number of measurement frequency	N = 14
RMS band width	ω_{RMS} = 8.8 X 10^7 rad/sec (14 MHz)
RF frequency	F =327 MHz
Error of cable delay difference (group delay)	$t_{BWS} = \sigma_\phi$ / SQRT(N) / ω_{RMS} = 530 psec.

We calculated the cable delay difference using the physical cable length difference (6910 m)for comparison. The calculated cable delay differences are summarized in Table 2. Taking account the 10-m resolution of the cable length measurement, we estimated the error of these calculated values to be 0.1 μsec.

4. Results

1) Power level check of the delay calibration signal

Table 3 shows the expected and observed signal level of the signal of S6. Except for the return link of the normal calibration signal, the observed signal levels of the normal calibration signal and the reflected calibration signal mostly agree with the expected value. The loss of the return link of the normal calibration signal is 10.5 dB lower than expected value. This loss is thought to be mainly caused by the loose connection of the optical connectors because the loss of the electric signal is proportional to the square of the optical signal loss.

We do not mention the S4 signal because there was trouble with the WDM and the signal level was not stable.

2) Delay calibration test

The delay calibration signals are reproduced from the data recorded by the DDR. The phase of the delay calibration signal of each frequency was measured by using the phase detector installed in the K4 input interface [(1)]. We estimated the cable delay differences by using a bandwidth synthesis technique that uses the measured phase. The estimated cable delay differences are summarized in Table 4.

It is thought that the instability of the signal level caused by the WDM trouble of the S4 link is the reason the phase residual is greater than expected phase error. The cable delay difference of the reflected signal corresponds to a 2-way cable delay difference of the optical signal with the wavelength of 1550 nm, while the cable delay difference of the normal calibration signal corresponds to the sum of the 1-way cable delay difference of the optical signal with a wavelength of 1310 nm and the optical signal with a wavelength of 1550 nm. Thus, the 2-way cable delay difference of the optical signal with the wavelength of 1310 nm was estimated to be 59,402.31 nsec. These estimated values are about 0.2 μsec smaller than the value calculated from the cable length difference.

5. Conclusions

We performed experiments for the delay compensation system using the GMRT. For the power level check, even though the results were almost the same as those expected, the return link of the normal calibration signal had a large loss which is thought to be caused by the loose connection of the optical connectors. For the delay calibration test, we measured cable delay differences using delay calibration signals and confirmed that the obtained cable delay differences were almost the same as the values calculated from the physical cable length. With regard to the link budget, these results show that our delay calibration method can be applied in cables longer than 20 km.

Applying this system to the KSP VLBI network, the delay determination accuracy improves because of the introduction of phase delay. It also decreases the vertical component error of the station position because the baseline analysis can be made without the need for estimating clock difference [(7)].

Acknowledgements

We would like to thank Prof. S. Ananthakrishnan and the staff of the GMRT for their

great help with the experiments. We are also grateful to Dr. Tetsuro Kondo of CRL for his useful information about data analysis.

References

(1) H. Kiuchi, M. Imae, T. Kondo, M. Sekido, S. Hama, T. Yamamoto, H. Uose, and T. Hoshino, "Real Time VLBI of the KSP," Proc. Technical Workshop for APT and APSG, pp. 125-129, 1996.
(2) T. Kondo, et al., ”Evaluation of repeatability of baseline length in the VLBI network around the Tokyo metropolitan area,” Geophysical Research Letters, vol. 25, no. 7, pp. 1047-1050, 1998.
(3) J. Amagai, et al., “Fundamental Experiments of Radio Interferometer using Fiberoptic Links Modulated in Radio Frequency” Proc. of TWAA, pp. 269-273, 1996.
(4) S. Ananthakrishnan, “Giant Meterwave Radio Telescope,” Proc. of TWAA, pp. 90-94, 1996.
(5) E. Iannone, et al., ”Nonlinear Optical Communication Networks,” Wiley-Interscience, New York, 1998.
(6) A. R. Whitney, “Precision geodesy and astrometry via very-long-baseline interferometry, “ Doctoral thesis for Massachusetts Institute of Technology, Jan. 1974.
(7) K. Heki, "Three Approaches to Improve the Estimation Accuracies of the Vertical VLBI Station Positions," J. of Geod. Soc. of Japan, vol. 36, no. 3, pp. 143-154, 1990.

Figure captions

Fig. 1 System configuration of the optical-linked RF interferometer.

Fig. 2 Configuration of the experiment that used the GMRT facilities.

Fig. 3 The locations of the 30 dishes of GMRT (taken from a GMRT pamphlet). S4 and S6 are the elements that are used in the experiment.

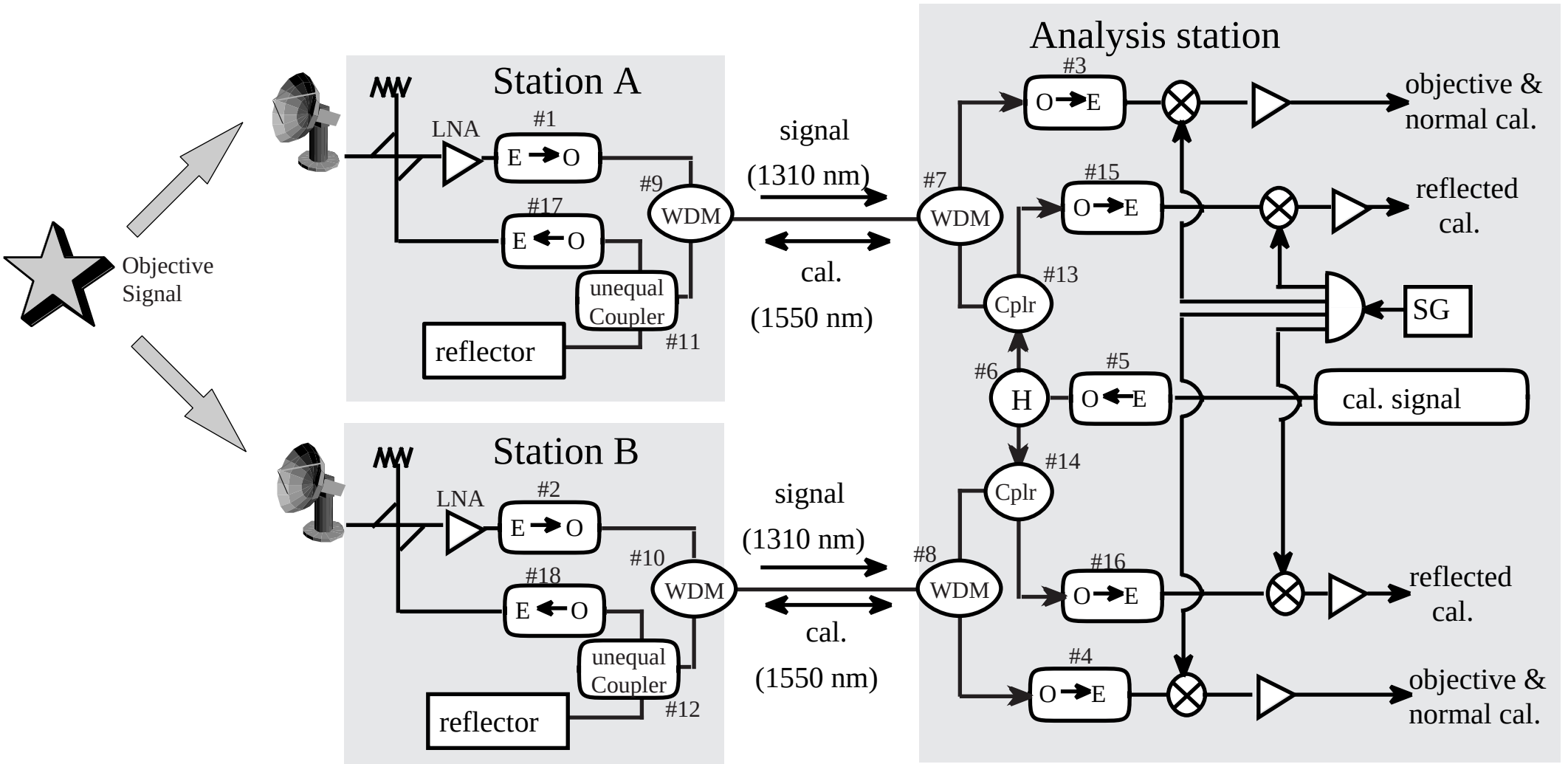
Analysis station
Station A
Station B
Objective
Signal
LNA
LNA
#1
#2
#3
#4
#5
#6
#7
#8
#9
#10
#11
#12
#13
#14
#15
#16
#17
#18
E → O
E ← O
O → E
O ← E
WDM
WDM
WDM
WDM
unequal
Coupler
unequal
Coupler
reflector
reflector
signal
(1310 nm)
cal.
(1550 nm)
signal
(1310 nm)
cal.
(1550 nm)
Cplr
Cplr
H
SG
cal. signal
objective &
normal cal.
reflected
cal.
reflected
cal.
objective &
normal cal.

Antenna Site

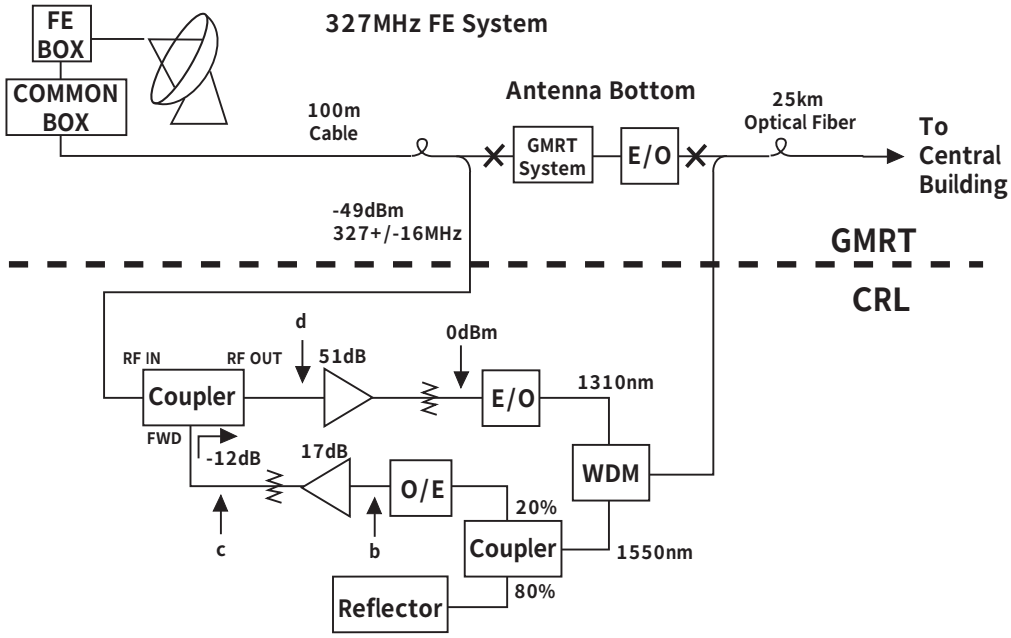

Central Building

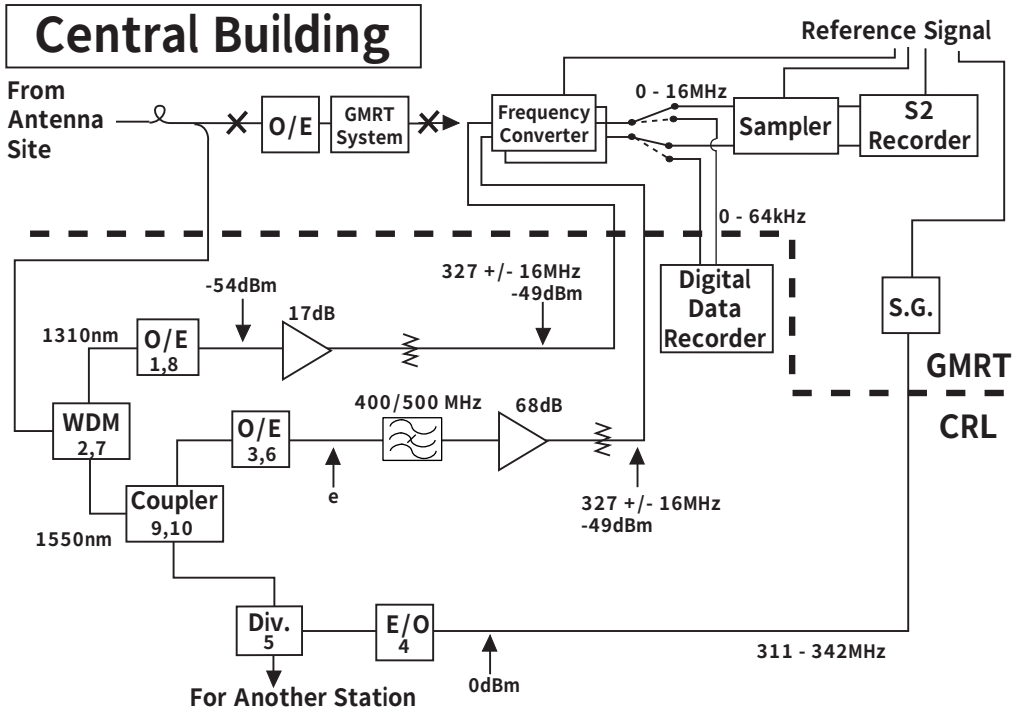

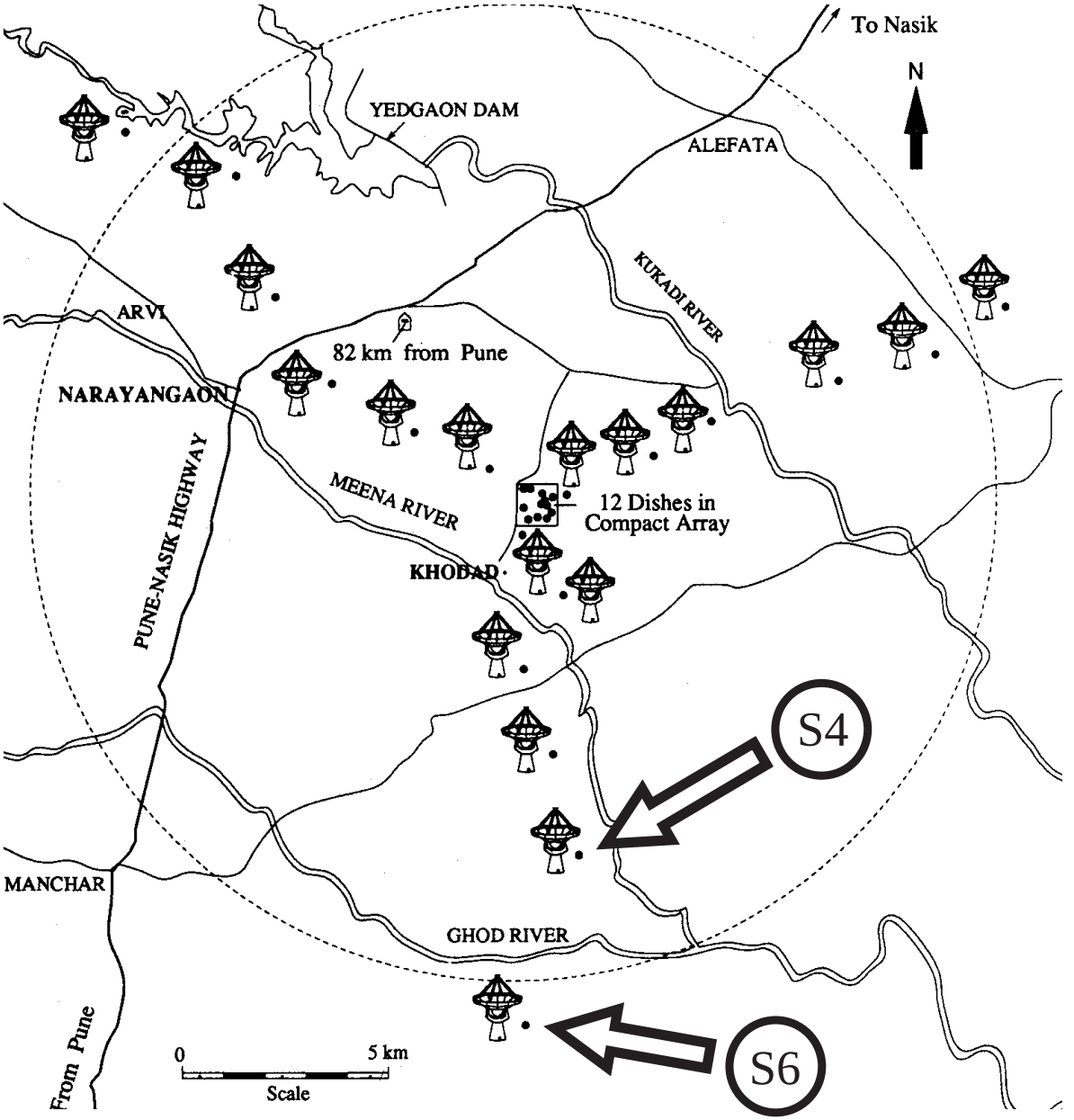
To Nasik
N
YEDGAON DAM
ALEFATA
KUKADI RIVER
ARVI
82 km from Pune
NARAYANGAON
PUNE-NASIK HIGHWAY
MEENA RIVER
12 Dishes in
Compact Array
KHODAD
S4
MANCHAR
GHOD RIVER
S6
From Pune
0
5 km
Scale

Table 1 The positions of the interferometer elements and the length of the optical fiber cables

		S4	S6
Position (WGS84)	(Latitude)	19° 0′ 26.9546″	18° 57′ 55.3542″
〃	(Longitude)	74° 3′ 33.4696″	74° 2′ 49.3453″
〃	(Height)	567.0483 m	610.6363 m
Cable length between elements and central building		13.75 km	19.94 km

Table 2 Calculated cable delay differences

wavelength[nm]	refractivity	2-way cable delay diff.[μsec]
1310	1.44692	-59.75
1550	1.44402	-59.63

Table 3 Link budget for S6 antenna

Reflected cal					
	Optical		Electric		
	loss	power	loss	power	obs'd
	dB	dBm	dB	dBm	dBm
pcal out		5.0		0.0	0.0
3dB divider	-3.5	1.5	-7.0	-7.0	
coupler	-3.5	-2.0	-7.0	-14.0	
WDM	-0.5	-2.5	-1.0	-15.0	
cable	-8.0	-10.5	-16.0	-31.0	
WDM	-0.5	-11.0	-1.0	-32.0	
unequal coupler(*)	-1.5	-12.5	-2.9	-34.9	
reflector	-0.5	-13.0	-1.0	-35.9	
unequal coupler(*)	-1.5	-14.4	-2.9	-38.9	
WDM	-0.5	-14.9	-1.0	-39.9	
cable	-8.0	-22.9	-16.0	-55.9	
WDM	-0.5	-23.4	-1.0	-56.9	
coupler	-3.5	-26.9	-7.0	-63.9	
opt system			-34.5	-98.4	
filter			-0.5	-98.9	
amp			68.0	-30.9	-32.0

Normal cal (forward)					
	Optical		Electric		
	loss	power	loss	power	obs'd
	dB	dBm	dB	dBm	
pcal out		5.0		0.0	0.0
3dB divider	-3.5	1.5	-7.0	-7.0	
coupler	-3.5	-2.0	-7.0	-14.0	
WDM	-0.5	-2.5	-1.0	-15.0	
cable	-8.0	-10.5	-16.0	-31.0	
WDM	-0.5	-11.0	-1.0	-32.0	
unequal coupler(*)	-7.5	-18.5	-15.0	-47.0	
opt system			-34.5	-81.5	-83.5

Normal cal (return)

	Optical loss dB	power dBm	Electric loss dB	power dBm	obs'd
				-84.0	-84.0
amp			51.0	-33.0	
attenuator		5.0	6.0	-27.0	
WDM	-0.5	4.5	-1.0	-28.0	
cable	-8.0	-3.5	-16.0	-44.0	
WDM	-0.5	-4.0	-1.0	-45.0	
opt system			-34.5	-79.5	
amp			17.0	-62.5	-71.0

Cable Loss

WL	1550	nm
length	19.9	km
loss/km	-0.40	dB/km
total loss	-8.0	dB

Coupler(*)

ratio	0.800

Table 4 Estimated cable difference

	Estimated cable delay difference[nsec]		
	BWS result [nsec]	ambiguity corrected [nsec]	Phase residual
Normal Cal.	691.73 +/- 0.65	-59,308.27 +/- 0.65	12.4 deg
Reflected cal.	785.77 +/- 0.93	-59,214.23 +/- 0.93	17.3 deg